

1    **Investigation of the Ice-Binding-Site of an Insect**

2    **Antifreeze Protein using Sum-Frequency Generation**

3    **Spectroscopy**

4    *Konrad Meister<sup>†</sup>\*, Stephan Lotze<sup>†</sup>, Luuk L. C. Olijve<sup>‡</sup>, Arthur L. DeVries<sup>§</sup>, John G. Duman<sup>#</sup>, Ilja*

5    *K. Voets<sup>‡</sup> & Huib J. Bakker<sup>†</sup>*

6    <sup>†</sup>FOM-Institute for Atomic and Molecular Physics AMOLF, Science Park 104, 1098 XG

7    Amsterdam, The Netherlands

8    <sup>‡</sup>Department of Chemical Engineering and Chemistry and Institute for Complex Molecular

9    Systems, Eindhoven University of Technology, 5600 MB Eindhoven, The Netherland

10    <sup>§</sup>Department of Animal Biology, University of Illinois at Urbana–Champaign, Urbana, IL,

11    61801, USA,

12    <sup>#</sup>Department of Biological Sciences, University of Notre Dame, Notre Dame, IN, 46556, USA

13    AUTHOR INFORMATION

14    **Corresponding Author**

15    \*K.Meister@amolf.nl

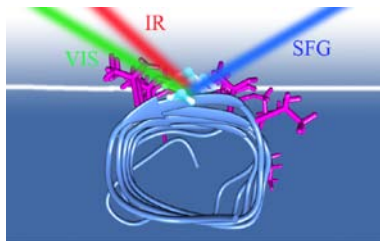
16 **Abstract:** We study the ice-binding site (IBS) of a hyperactive antifreeze protein from the beetle  
17 *Dendroides canadensis* (DAFP-1) using vibrational sum-frequency generation spectroscopy. We  
18 find that DAFP-1 accumulates at the air-water interface due to the hydrophobic character of its  
19 threonine-rich ice-binding site, while retaining its highly regular  $\beta$ -helical fold. We observe a  
20 narrow band at  $3485\text{ cm}^{-1}$  that we assign to the O-H stretch vibration of threonine hydroxyl  
21 groups of the ice-binding site. The narrow character of the  $3485\text{ cm}^{-1}$  band suggests that the  
22 hydrogen bonds between the threonine residues at the IBS and adjacent water molecules are  
23 quite similar in strength, indicating that the IBS of DAFP-1 is extremely well ordered, with the  
24 threonine side chains showing identical rotameric confirmations. The hydrogen-bonded water  
25 molecules do not form an ordered ice-like layer, as was recently observed for the moderate  
26 antifreeze protein type III (AFP-III). It thus appears that the antifreeze action of DAFP-1 does  
27 not require the presence of ordered water, but likely results from the direct binding of its highly  
28 ordered array of threonine residues to the ice surface.

29

30

31

32



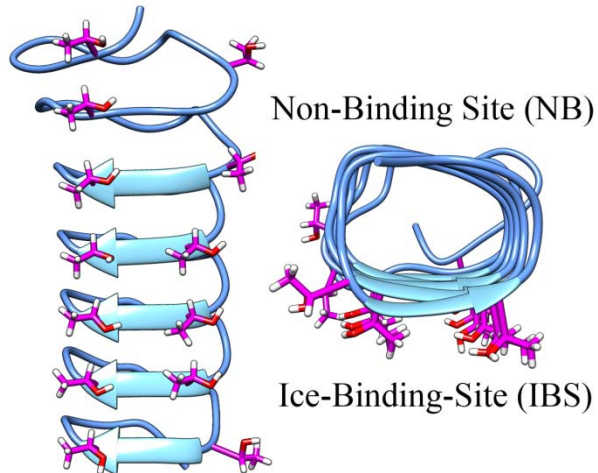
33

34

35    **KEYWORDS** Antifreeze Proteins, Chiral Sum-Frequency Generation Spectroscopy, Phase-  
36    Sensitive Sum-Frequency Generation, Air-Water Interface, Protein-Water Interface

37

38 Antifreeze proteins (AFPs) have been isolated and structurally characterized from a wide range  
39 of organisms, including bacteria, plants, fungi, insects and polar fish<sup>1,2</sup>. Despite their structural  
40 heterogeneity and differences in activity, all AFPs are believed to function by an adsorption-  
41 inhibition mechanism in which the proteins recognize and irreversibly bind to the surface of  
42 small ice crystallites thereby preventing further growth of the crystallites at the adsorbed  
43 positions<sup>3</sup>. As a result, ice growth is limited to regions between adsorbed AFPs, and thus the ice  
44 is forced to grow in energetically unfavorable curved fronts. This effect eventually leads to the  
45 termination of crystal growth, and lowers the freezing point, a phenomenon known as the Kelvin  
46 effect. Ice binding involves a particular region of the antifreeze protein known as the ice-  
47 binding-site (IBS). Ice-binding-sites are usually relatively flat, hydrophobic and contain almost  
48 no charged residues. Molecular dynamics simulations provided evidence on the existence of  
49 preordered ice-like water molecules and/or decelerated water dynamics around the IBS of  
50 several AFPs, pointing towards an active involvement of water in their mode of action<sup>4-6</sup>.  
51 However, given the fact that AFPs bind ice nuclei in an environment that is largely liquid water  
52 makes it experimentally challenging to determine the structure and dynamics of the protein  
53 hydration shell. Consequently, up to now the mechanism of recognition and initial binding has  
54 barely been studied experimentally. We recently studied the properties of water hydrating the  
55 ice-binding site of AFP-III with vibrational sum-frequency generation (VSFG)<sup>7</sup>. This technique  
56 is ideally suited for this study as it is highly selective for molecules residing at interfaces.



57

58 **Figure 1.** Model of the 3D-structure of the insect antifreeze protein DAFP-1. DAFP-1 consists  
 59 of seven identical repeats that form an exceptional regular right-handed  $\beta$ - helix. The ice-  
 60 binding-site consists of a flat, relatively hydrophobic and threonine-rich surface.

61 DAFP-1 consists of several identical 13-aa repeats that form a right-handed  $\beta$ -helix fold as  
 62 seen in figure 1. The helix is stabilized by disulfide bonds and an extensive H-bond network,  
 63 thus creating probably one of the most regular protein structures known<sup>8</sup>. The ice-binding site of  
 64 this protein has been identified as a relatively flat, hydrophobic  $\beta$ -sheet that consists of two rows  
 65 of threonine residues adjacent to a narrow trough. Several regularly spaced water molecules, H-  
 66 bonded to the hydroxyl groups of the threonines, were observed in the crystal structure of a  
 67 *Tenebrio molitor* AFP (TmAFP), a structural homolog of DAFP-1<sup>9</sup>. Molecular dynamics (MD)  
 68 simulations confirmed the existence of regularly arranged water molecules at the surface, and  
 69 showed that these water molecules remain associated with the protein in solution, thus  
 70 constituting part of the AFP<sup>6</sup>. Further MD-simulations and Terahertz spectroscopic studies  
 71 identified several layers of slowed hydrogen-bond dynamics of water sets of periodically  
 72 arranged ordered water molecules parallel to the ice-binding site of the protein<sup>5,10</sup>. Contrasting

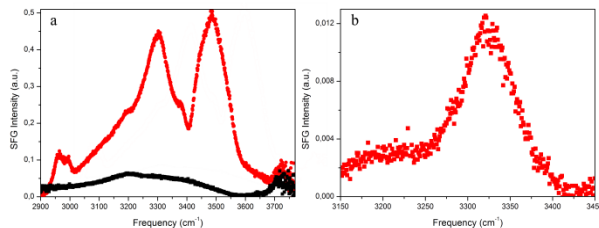
73 with these findings is a NMR study which found no indication for ice-like water or the presence  
74 of an extended hydration shell<sup>11</sup>.

75 In this work we study the properties of the ice-binding site of DAFP-1 and the adjacent water  
76 molecules using a combination of different sum-frequency generation techniques. In VSFG an  
77 infra-red light pulse and a visible pulse are combined at an interface to generate light at their  
78 sum-frequency. The generation is enhanced in case the infrared light is resonant with a molecular  
79 vibration. For most systems the generation of sum-frequency light is symmetry-forbidden in the  
80 bulk which makes VSFG highly surface specific. By interfering the VSFG signal from the  
81 sample with a reference sum-frequency field, we determine the phase of the generated sum-  
82 frequency light, and thereby the phase of the second-order optical susceptibility  $\chi^{(2)}$ . The real  
83 (Re) and imaginary (Im) parts of  $\chi^{(2)}$  provide direct information on the orientation of the  
84 vibrational transition dipole moments at the surface<sup>12</sup>. This phase-sensitive VSFG thus provides  
85 information that is not obtained in conventional intensity VSFG as the signal measured with this  
86 technique is proportional to  $|\chi^{(2)}|^2$ . VSFG and phase-sensitive VSFG (PS-VSFG) have been  
87 successfully applied to identify the orientation of interfacial water molecules next to various  
88 biomolecules<sup>13,14</sup>.

89 We determined the surface propensity of DAFP-1 by measuring the surface tension of aqueous  
90 solutions containing different concentrations of the protein. We observed surface tensions of 45-  
91 60 mN/m, depending on the DAFP-1 concentration. This surface tension is significantly lower  
92 than the surface tension of ~72 mN/m of pure liquid water from which we conclude that DAFP-1  
93 is a surface active molecule, comparable to AFP-III<sup>15</sup>. The IBS of DAFP-1 is quite hydrophobic,  
94 while the other surfaces of the protein are dominantly hydrophilic, making DAFP-1 an

95 amphiphilic system (FigS1). As a result, DAFP-1 proteins at the water-air interface will likely be  
96 oriented with their IBS towards the air phase and their hydrophilic surfaces to the water face<sup>16</sup>.

97 Figure 2a shows the VSFG spectrum of the interface of pure liquid water ( $\text{H}_2\text{O}$ ) and of a 20  
98  $\mu\text{M}$  DAFP-1 solution (pH 7.5), both at room temperature ( $20^\circ\text{C}$ ). The VSFG spectrum of the  
99 water-air interface (in black) shows a broad double-peaked band between  $\sim 3100$  and  $\sim 3600\text{ cm}^{-1}$ .  
100 This broad band is associated with the O-H stretch vibrations of  $\text{H}_2\text{O}$  molecules forming  
101 hydrogen bonds to other  $\text{H}_2\text{O}$  molecules. The spectrum also shows a relatively narrow band at  
102  $\sim 3730\text{ cm}^{-1}$  that can be assigned to the OH-stretch vibrations of non-hydrogen bonded OH  
103 groups that are sticking out of the surface<sup>17</sup>. All spectra shown are background subtracted and  
104 normalized with respect to a reference SFG spectrum.



105  
106 **Figure 2.** VSFG spectra of pure water (black) and a 20  $\mu\text{M}$  DAFP-1 solution (pH 7.5) (red) at  
107 the air-water interface, measured in ssp and psp polarization configuration. (a) The VSFG  
108 spectrum of DAFP-1 (in red) in ssp shows several contributions belonging to CH-, NH- and OH-  
109 stretching vibrations. Among them are two sharp bands at  $\sim 3300\text{ cm}^{-1}$  and  $\sim 3485\text{ cm}^{-1}$ . (b) In the  
110 psp spectrum of DAFP-1 a single peak at  $\sim 3320\text{ cm}^{-1}$  is observed that we assign to the N-H  
111 stretch vibration of the chiral,  $\beta$ -helical fold of DAFP-1.

112 The VSFG spectrum of the aqueous DAFP-1 solution (in red) also shows a broad response in  
113 the spectral region of the O-H stretch vibrations and bands that can be assigned to methylene and

114 methyl vibrations ( $2880 - 3000 \text{ cm}^{-1}$ ). At frequencies  $> 3100 \text{ cm}^{-1}$  the VSFG spectrum of the  
115 DAFP-1 solution shows two strong, relatively narrow bands at  $\sim 3300 \text{ cm}^{-1}$  (FMHW  $\sim 65 \text{ cm}^{-1}$ )  
116 and  $\sim 3485 \text{ cm}^{-1}$  (FMHW  $\sim 95 \text{ cm}^{-1}$ ). We assign these bands to protein specific signals. This  
117 frequency region also shows weaker bands at  $3200 \text{ cm}^{-1}$ ,  $3380 \text{ cm}^{-1}$  and  $3730 \text{ cm}^{-1}$  that we assign  
118 to water background signals. Previous VSFG studies of non-AF protein solutions also showed  
119 the presence of a narrow peak at  $3300 \text{ cm}^{-1}$ . This peak was assigned to either the amide A mode  
120 related to the protein backbone or to side-chain related amine resonances<sup>18-20</sup>. Both assignments  
121 are possible for DAFP-1. The VSFG spectra of Fig. 2 are measured in ssp polarization  
122 configuration (s-polarized SFG, s-polarized visible and p-polarized infrared), and this  
123 polarization configuration does not allow for a distinction between the two possible assignments.

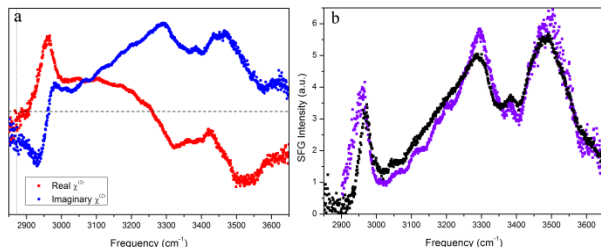
124 In order to determine the molecular origin of the signal at  $3300 \text{ cm}^{-1}$  we performed chiral  
125 VSFG-measurements using a psp polarization configuration (p-polarized SFG, s-polarized  
126 visible and p-polarized infrared). Chiral VSFG has been used before to determine the secondary  
127 structures of proteins at interfaces as it is highly selective for signals from macromolecules with  
128 a chiral architecture<sup>21</sup>. In Figure 2b we show the VSFG spectrum of DAFP-1 in psp polarization.  
129 This spectrum shows a narrow band at  $3320 \text{ cm}^{-1}$  that can be unambiguously assigned to the N-H  
130 vibrations of the helical protein backbone of DAFP-1<sup>19,20</sup>. The observation of a chiral VSFG  
131 signal demonstrates that DAFP-1 remains in its regular  $\beta$ -helical fold, since unfolding of the  
132 helix at the interface would eliminate the chirality and consequently the psp VSFG signal. In  
133 view of the clear presence of the N-H vibrations of the helical protein backbone in the psp VSFG  
134 spectrum, the band at  $3300 \text{ cm}^{-1}$  in the ssp spectrum likely has the same origin.

135 The other narrow band observed in the ssp spectrum of Fig. 2 at  $\sim 3485 \text{ cm}^{-1}$  has not been  
136 observed before in VSFG spectra of proteins. We exclude further contributions from N-H

137 vibrations since these vibrations are expected to have lower frequencies. Hence, the narrow band  
138 at 3485 cm<sup>-1</sup> is likely associated with the O-H vibration of particular amino acid residues or  
139 water molecules adsorbed at the protein surface.

140 In previous infrared spectroscopic studies of hydrogen-bonded alcohol clusters, a vibrational  
141 signal at ~3500 cm<sup>-1</sup> has been assigned to the O-H stretch vibration of an alcohol molecule that  
142 is donating but not accepting a hydrogen-bond<sup>22,23</sup>. Previous VSFG studies have assigned signals  
143 at ~3500 cm<sup>-1</sup> to alcohol dimers and carbohydrate-water systems<sup>24,25</sup>, which also constitute  
144 systems in which an O-H group of an organic molecule is only donating and not accepting a  
145 hydrogen bond. Threonine possesses an alcoholic O-H group, and thus is an amino-acid that  
146 complies with these characteristics. Moreover, threonine residues are abundantly present in  
147 DAFP-1, especially at the IBS. DAFP-1 consists of nearly 20% of threonine and within the IBS  
148 more than 60% of the residues are threonine<sup>8</sup>. Furthermore, 7 of the 11 threonine residues in the  
149 IBS have been proposed to form a strong hydrogen-bond with a fixed water molecule<sup>9</sup>. We  
150 therefore assign the band at 3485 cm<sup>-1</sup> to the O-H stretch vibrations of the hydroxyl groups of  
151 threonine that donate hydrogen bonds to water molecules. The frequency of 3485 cm<sup>-1</sup> is  
152 somewhat lower than the frequency of 3500-3520 cm<sup>-1</sup> of the O-H stretch vibration of the last  
153 hydroxyl group donating a hydrogen bond in a hydrogen-bonded cluster of alcohol  
154 molecules<sup>21,22</sup>, indicating that the hydrogen bond donated by the hydroxyl group of threonine is  
155 relatively strong. However, the frequency of 3485 cm<sup>-1</sup> is high compared to the center of the  
156 absorption band of the O-H stretch vibrations of liquid HDO:D<sub>2</sub>O, indicating that the hydrogen  
157 bond donated by the hydroxyl group of threonine is weaker than the average hydrogen bond in  
158 water. In bulk water the hydrogen bonds constitute extended conjugated hydrogen-bond  
159 networks, and this conjugation makes the hydrogen bonds stronger. The width of ~95 cm<sup>-1</sup> of the

160 threonine OH peak is much narrower than the spectral width of  $\sim 300$   $\text{cm}^{-1}$  of the O-H stretch  
161 absorption bands of alcohol clusters and of HDO:D<sub>2</sub>O. The large bandwidth of the latter systems  
162 results from the large variation in structures and hydrogen-bond strengths. The much smaller  
163 width of the threonine OH peak shows that the hydrogen bonds donated by the threonine  
164 residues have a quite well-defined strength. This finding implies that the IBS of DAFP-1 would  
165 be well ordered, with the threonine side chains showing motional rigidity and identical rotameric  
166 conformations<sup>26,27</sup>.



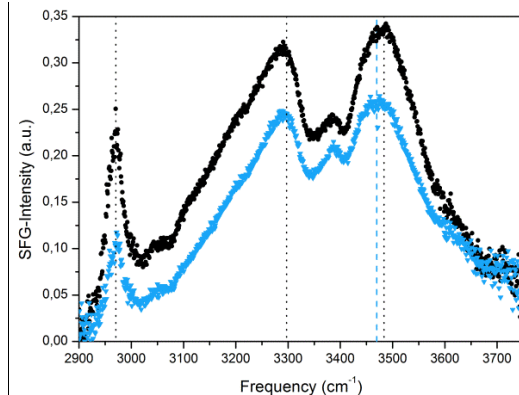
167

168 **Figure 3.** (a) Real and Imaginary  $\chi(2)$  of a 40  $\mu\text{M}$  DAFP-1 (pH 7.5) solution at the air-water  
169 interface measured with ssp polarization. (b)  $(\text{Im } \chi^{(2)})^2 + (\text{Re } \chi^{(2)})^2$  (purple) and conventional  
170 VSFG spectrum of 40  $\mu\text{M}$  DAFP-1.

171 To further elucidate the absolute orientation of DAFP-1, threonine and its surrounding  
172 interfacial water, we performed PS-VSFG measurements. Figure 3a shows the PS-VSFG  
173 spectrum of a 40  $\mu\text{M}$  DAFP-1 solution (pH 7.5) at room temperature (20°C). In Figure 3b we  
174 compare  $|\chi^{(2)}|^2$  constructed from the PS-VSFG data with the conventional VSFG spectrum. The  
175 two spectra are in excellent agreement, thus validating the PS-VSFG spectrum. The PS-VSFG  
176 spectrum shows two negative bands at  $\sim 2880$   $\text{cm}^{-1}$  and  $\sim 2940$   $\text{cm}^{-1}$  that can be assigned to the  
177 methyl symmetric stretching ( $\text{CH}_3,\text{ss}$ ) and methyl Fermi resonance ( $\text{CH}_3,\text{FR}$ ), respectively<sup>13</sup>. A  
178 positive band with a maximum at  $\sim 2975$   $\text{cm}^{-1}$  can be assigned to the methyl antisymmetric

179 stretching vibration ( $\text{CH}_{3,\text{AS}}$ ). The negative signs of the  $\text{CH}_{3,\text{SS}}$  and  $\text{CH}_{3,\text{FR}}$  bands and the positive  
180 sign of  $\text{CH}_{3,\text{AS}}$  indicate the presence of terminal methyl CHs oriented towards the air<sup>14</sup>. DAFP-  
181 I's ice-binding site is rather flat and consists almost entirely of threonine residues, as seen in  
182 figure 1. As a result, the upward facing methyl groups are likely associated with the side chains  
183 of threonine residues. The  $\text{Im}\chi^{(2)}$  spectrum of DAFP-I shows two distinct positive peaks at  $\sim 3300$   
184  $\text{cm}^{-1}$  and  $\sim 3500 \text{ cm}^{-1}$ . The positive sign of the latter peak implies that the threonine O-H groups  
185 are also pointing towards the air. The PS-VSFG spectrum thus shows that the threonine side  
186 chains are pointing up, in agreement with the conformation of a TmAFP dimer that was found in  
187 low-temperature X-ray diffraction studies<sup>9</sup>. Here we observe this conformation for a single  
188 DAFP-1 in the aqueous phase at room temperature.

189 In Figure 4 we compare VSFG spectra of DAFP-1 measured at  $20^\circ \text{ C}$  and  $0^\circ \text{ C}$ . The similarity  
190 of the two VSFG spectra of Figure 4 shows that no significant structural change occurs upon  
191 lowering the temperature. Decreasing the temperature appears to lead only to a small decrease of  
192 the intensity of the VSFG spectrum and a small red shift of the threonine O-H band. The red shift  
193 indicates that the hydrogen bond donated by the threonine hydroxyl group to water becomes  
194 slightly stronger when the temperature is decreased. This is a quite common observation for  
195 hydrogen-bonded systems. We conclude that lowering the temperature enhances the hydrogen  
196 bonding but has little effect on the secondary structure of DAFP-1, as suggested before by  
197 circular dichroism and linear infrared spectroscopy<sup>28</sup>.



198

199 **Figure 4.** VSFG spectra of a 40  $\mu\text{M}$  DAFP-1 solution (pH 7.5) at 20° C (black) and 0° C  
 200 (blue). Lowering the temperature enhances hydrogen bonding and leads to a red shift of the  
 201 threonine OH signal and a decrease of the amplitude. The dashed vertical lines indicate the  
 202 central frequency positions of the threonine OH bands at the two different temperatures.

203 We study the properties of the hyperactive insect antifreeze protein DAFP-1 with  
 204 conventional, chiral and phase-resolved vibrational surface sum-frequency generation. We  
 205 observe that DAFP-1 accumulates at the air-water interface, probably as a result of the  
 206 predominantly hydrophobic character of the threonine-rich IBS. Owing to its particular regular  
 207  $\beta$ -helical structure, contributions arising from N-H stretching vibrations of the chiral protein  
 208 backbone could clearly be assigned, confirming that DAFP-1 does not undergo structural  
 209 changes or unfolding upon adsorption to the interface. The VSFG spectrum of DAFP-1 shows a  
 210 strong narrow band at 3485  $\text{cm}^{-1}$  that we assign to the hydroxyl groups of threonine residues  
 211 located at the ice-binding site that donate hydrogen bonds to water molecules. The narrow  
 212 character of the 3485  $\text{cm}^{-1}$  band indicates that the hydrogen bonds between the threonine residues  
 213 at the IBS and the water molecules are quite similar in strength, indicating that the IBS of DAFP-  
 214 1 is extremely well ordered, with the threonine side chains showing identical rotameric  
 215 confirmations. Using PS-VSFG measurements we were able to determine the absolute

216 orientation of the threonine side chains of DAFP-1 with both the terminal methyl and hydroxyl  
217 group pointing up.

218 In a recent study of AFP-III we observed that the O-H stretch vibrational spectrum of water to  
219 the IBS has the form of a relatively narrow peak at  $\sim 3250 \text{ cm}^{-1}$ , quite similar to the O-H stretch  
220 vibrational spectrum of water ice<sup>7</sup>. This observation supports an ice-binding mechanism of AFP-  
221 III in which the IBS has a high affinity for ice surfaces thanks to the ice-like character of its  
222 hydration shell. The VSFG spectrum measured for DAFP-1 does not show the presence of such  
223 highly structured ice-like water layers. The VSFG spectrum is in fact dominated by the O-H  
224 stretch vibration of threonine residues that donate hydrogen bonds to adsorbed water molecules.  
225 This difference in VSFG spectra between DAFP-1 and AFP-III indicates that the water adsorbed  
226 to the IBS of DAFP-1 is of quite different character than the water adsorbed to the IBS of AFP-  
227 III<sup>7</sup>. It was observed in a crystallographic study on the related MpAFP that the water molecules  
228 bound to the IBS are quite regularly positioned<sup>29</sup>. The regular positioning is likely due to the fact  
229 that the water molecules accept hydrogen bonds from the hydroxyl groups of a highly ordered  
230 array of threonine residues. It should be noted that the regular positioning of the water molecules  
231 does not imply that the water molecules themselves would be donating strong hydrogen bonds to  
232 other water molecules. In the crystallographic study on MpAFP the authors speculate that in  
233 solution water near the IBS is likely very mobile<sup>29</sup>. Here we find strong evidence that this is  
234 indeed the case, as the water molecules are observed not to form a well-ordered ice-like layer.

235 The IBS of DAFP-1 consists of a well-ordered array of threonine residues that already by itself  
236 provides a good surface similarity to ice. Consequently it seems that DAFP-1 does not require  
237 additional ordered water layers to obtain a high ice-surface affinity. In contrast to that, AFP-III  
238 consists of no repetitive sequence or structural match on its surface and would require stable

239 water layers to provide a structural match to the ice-plane. We speculate that different water  
240 layers for moderate and hyperactive AFPs might actually be a mandatory requirement in order to  
241 be able to distinguish and bind to different planes of ice, which themselves have different growth  
242 rates and orientations of water molecules. For instance, the more disordered water at the IBS of  
243 DAFP-1 may provide sufficient malleability for docking onto two distinct ice crystal planes.  
244 Moreover, if ice-binding requires solidification of hydration water at the IBS, this may also be  
245 faster for preformed ice-like water associated with AFP-III than for the more disordered surface  
246 water of DAFP-1. This could explain the more pronounced time-dependent activity for DAFP-1  
247 compared to AFP-III, as was recently reported<sup>30</sup>.

248 Summarizing, we used a combination of VSFG, chiral and phase-sensitive vibrational sum-  
249 frequency generation spectroscopy to investigate the ice-binding site of the hyperactive  
250 antifreeze protein DAFP-1. The VSFG spectra reveal that the IBS of DAFP-1 is extremely well  
251 ordered, with the threonine side chains showing identical rotameric confirmations. Using PS-  
252 VSFG measurements we were able to determine the absolute orientation of the threonine side  
253 chains of DAFP-1 and we found that both the terminal methyl and hydroxyl group are pointing  
254 up. Our findings reveal that moderate and hyperactive AFPs have structurally different IBS and  
255 hydration layers, which are likely optimized to their specific task.

256 ASSOCIATED CONTENT

257 AUTHOR INFORMATION

258 **Corresponding Author**

259 \*Email: K.Meister@amolf.nl

260 **Notes**

261 The authors declare no competing financial interests.

262 **ACKNOWLEDGMENT**

263 This work is part of the research program of the Stichting voor Fundamenteel Onderzoek der  
264 Materie, which is financially supported by the Nederlandse Organisatie voor Wetenschappelijk  
265 Onderzoek (NWO). I.K.V. is grateful for financial support from NWO (Veni Grant 700.10.406)  
266 and the European Union (FP7-PEOPLE-2011-CIG Contract 293788 and FP7-PEOPLE-2012-  
267 ITN Contract 316866).

268

269 **SUPPORTING INFORMATION (SI)**

270 **Supporting Information Available:** Experimental Details, Figures S1-S3. This material is  
271 available free of charge via the internet <http://pubs.acs.org>.

272

273

274 **REFERENCES**

275

276 (1) DeVries, A. L. Glycoproteins as Biological Antifreeze Agents in Antarctic Fishes. *Science*  
277 **1971**, *172*, 1152-1155.

278 (2) Duman, J. G. Antifreeze and Ice Nucleator Proteins in Terrestrial Arthropods. *Annu. Rev.*  
279 *Physiol.* **2001**, *63*, 327-355.

280 (3) Raymond, J. A.; DeVries, A. L. Adsorption Inhibition as a Mechanism of Freezing  
281 Resistance in Polar Fishes. *Proc. Natl. Acad. Sci. USA* **1977**, *74*, 2589-2593.

282 (4) Nutt, D. R.; Smith, J. C. Dual Function of the Hydration Layer around an Antifreeze Protein  
283 Revealed by Atomistic Molecular Dynamics Simulations. *J. Am. Chem. Soc.* **2008**, *130*, 13066-  
284 13073.

285 (5) Midya, U. S.; Bandyopadhyay, S. Hydration Behavior at the Ice-Binding Surface of the  
286 *Tenebrio molitor* Antifreeze Protein. *J. Phys. Chem. B.* **2014**, *118*, 4743-4752.

287 (6) Yang, Z.; Zhou, Y.; Liu, K.; Cheng, Y.; Liu, R.; Chen, G.; Jia, Z. Computational Study on the  
288 Function of Water within a Beta-Helix Antifreeze Protein Dimer and in the Process of Ice-  
289 Protein Binding. *Biophys J.* **2003**, *85*, 2599-2605.

290 (7) Meister, K.; Strazdaite, S.; DeVries, A. L.; Lotze, S.; Olijve, L. L. C.; Voets, I. K.; Bakker,  
291 H. J. Observation of Ice-Like Water Layers at an Aqueous Protein Surface. *Proc. Natl. Acad. Sci.*  
292 *USA* **2014**, *111*, 11372-11376.

293 (8) Wang, S.; Amornwittawat, N.; Juwita, V.; Kao, Y.; Duman, J. G.; Pascal, T. A.; Goddard, W.  
294 A.; Wen, X. Arginine, a Key Residue for the Enhancing Ability of an Antifreeze Protein of the  
295 Beetle *Dendroides Canadensis*. *Biochemistry* **2009**, *48*, 9696-9703.

296 (9) Liou, Y. C.; Tocilj, A.; Davies, P. L.; Jia, Z. Mimicry of Ice Structure by Surface Hydroxyls  
297 and Water of a Beta-Helix Antifreeze Protein. *Nature* **2000**, *406*, 322-324.

298 (10) Meister, K.; Ebbinghaus, S.; Xu, Y.; Duman, J. G.; DeVries, A.; Gruebele, M.; Leitner, D.  
299 M.; Havenith, M. Long-Range Protein-Water Dynamics in Hyperactive Insect Antifreeze  
300 Proteins. *Proc. Natl. Acad. Sci. USA* **2013**, *110*, 1617-1622.

301 (11) Modig, K.; Qvist, J.; Marshall, C. B.; Davies, P. L.; Halle, B. High Water Mobility on the  
302 Ice-Binding Surface of a Hyperactive Antifreeze Protein. *Phys. Chem. Chem. Phys.* **2010**, *12*,  
303 10189-10197.

304 (12) Shen, Y. R. Annu. Phase-Sensitive Sum-Frequency Spectroscopy. *Rev. Phys. Chem.* **2013**,  
305 *64*, 129-150.

306 (13) Engelhardt, K.; Peukert, W.; Braunschweig, B. Vibrational Sum-Frequency Generation at  
307 Protein Modified Air-Water Interfaces: Effects of Molecular Structure and Surface Charging.  
308 *Curr. Opin. Colloid Interface Sci.* **2014**, *19*, 207-215.

309 (14) Mondal, J. A.; Nihonyanagi, S.; Yamaguchi, S.; Tahara, T. Structure and Orientation of  
310 Water at Charged Lipid Monolayer/Water Interfaces Probed by Heterodyne-Detected Vibrational  
311 Sum Frequency Generation Spectroscopy. *J. Am. Chem. Soc.* **2010**, *132*, 10656-10657.

312 (15) Salvay, A. G.; Gabel, F.; Pucci, B.; Santos, J.; Howard, E. I.; Ebel, C. Structure and  
313 Interactions of Fish Type III Antifreeze Protein in Solution. *Biophys J.* **2010**, *99*, 609-618.

314 (16) Chandler, D. Interfaces and the Driving Force of Hydrophobic Assembly. *Nature* **2005**, *437*,  
315 640-647.

316 (17) Du, Q.; Superfine, R.; Freysz, E.; Shen, Y. R. Vibrational Spectroscopy of Water at the  
317 Vapor/Water Interface. *Phys. Rev. Lett.* **1993**, *70*, 2313-2136.

318 (18) Weidner, T.; Breen, N. F.; Drobny, G. P.; Castner, D. G. Amide or Amine: Determining the  
319 Origin of the  $3300\text{ cm}^{-1}$  NH Mode in Protein SFG Spectra Using  $^{15}\text{N}$  Isotope Labels. *J. Phys.*  
320 *Chem. B* **2009**, *113*, 15423-15426.

321 (19) Fu L.; Liu J.; Yan, E. C. Y. Chiral Sum Frequency Generation Spectroscopy for  
322 Characterizing Protein Secondary Structures at Interfaces *J. Am. Chem. Soc.* **2011**, *133*, 8094–  
323 8097.

324 (20) Fu, L.; Wang, Z.; Yan, E. C. Y. N-H Stretching Modes around 3300 Wavenumber from  
325 Peptide Backbones Observed by Chiral Sum Frequency Generation Vibrational Spectroscopy.  
326 *Chirality* **2014**, *26*, 521-524.

327 (21) Yan, E. C. Y.; Fu, L.; Wang, Z.; Liu, W. Biological Macromolecules at Interfaces Probed by  
328 Chiral Vibrational Sum Frequency Generation Spectroscopy. *Chem. Rev.* **2014**, *114*, 8471-8498.

329 (22) Gaffney, K. J.; Davis, P. H.; Piletic, I. R.; Levinger, N. E.; Fayer, M. D. Hydrogen Bond  
330 Dissociation and Reformation in Methanol Oligomers Following Hydroxyl Stretch Relaxation. *J.*  
331 *Phys. Chem. A* **2002**, *106*, 12012-12023.

332 (23) Graener, H.; Ye, T. Q.; Laubereau, A. Ultrafast Vibrational Predisociation of Hydrogen  
333 Bonds Mode Selective Infrared Photochemistry in Liquids. *J. Chem. Phys.* **1989**, *91*, 1043-1046.

334 (24) Laß, K.; Friedrichs, G. J. Revealing Structural Properties of the Marine Nanolayer from  
335 Vibrational Sum Frequency Generation Spectra. *Geophys. Res. Oceans* **2011**, *116*, C08042.

336 (25) Superfine, R., Nonlinear Spectroscopic Studies of Interfacial Molecular Ordering;  
337 University of California, Berkeley, USA; 1991.

338 (26) Daley, M. E.; Sykes, B. D. The Role of Side Chain Conformational Flexibility in Surface  
339 Recognition by *Tenebrio Molitor* Antifreeze Protein. *Protein Sci.* **2003**, *12*, 1323-1331.

340 (27) Daley, M. E.; Sykes, B. D. Characterization of Threonine Side Chain Dynamics in an  
341 Antifreeze Protein Using Natural Abundance  $^{13}\text{C}$  NMR Spectroscopy. *J. Biomol. NMR* **2004**, *29*,  
342 139-150.

343 (28) Li, N.; Kendrick, B. S.; Manning, M. C.; Carpenter, J. F.; Duman, J. G. Secondary Structure  
344 of Antifreeze Proteins from Overwintering Larvae of the Beetle *Dendroides Canadensis*. *Arch.*  
345 *Biochem. Biophys.* **1998**, *360*, 25-32.

346 (29) Garnham, C. P.; Campell, R. L.; Davies, P. L. Anchored Clathrate Waters Bind Antifreeze  
347 Proteins to Ice. *Proc. Natl. Acad. Sci. USA* **2011**, *108*, 7363-7367.

348 (30) Drori, R.; Celik, Y.; Davies, P. L.; Braslavsky, I. Ice-Binding Proteins that Accumulate on  
349 Different Ice Crystal Planes Produce Distinct Thermal Hysteresis Dynamics. *J R Soc Interface*  
350 **2014**, *11*, 0526.

351